Acute pharmacological inhibition of matrix metalloproteinase-9 activity during development restores perineuronal net formation and normalizes auditory processing in *Fmr1* KO mice

Patricia S. Pirbhoy[1], Maham Rais[1], Jonathan W. Lovelace[2], Walker Woodard[1], Khaleel A. Razak[2], Devin K. Binder[1], Iryna M. Ethell[1]

[1] Division of Biomedical Sciences, School of Medicine, University of California, Riverside Riverside, California 92521, USA

[2] Department of Psychology, University of California Riverside, Riverside, California 92521, USA

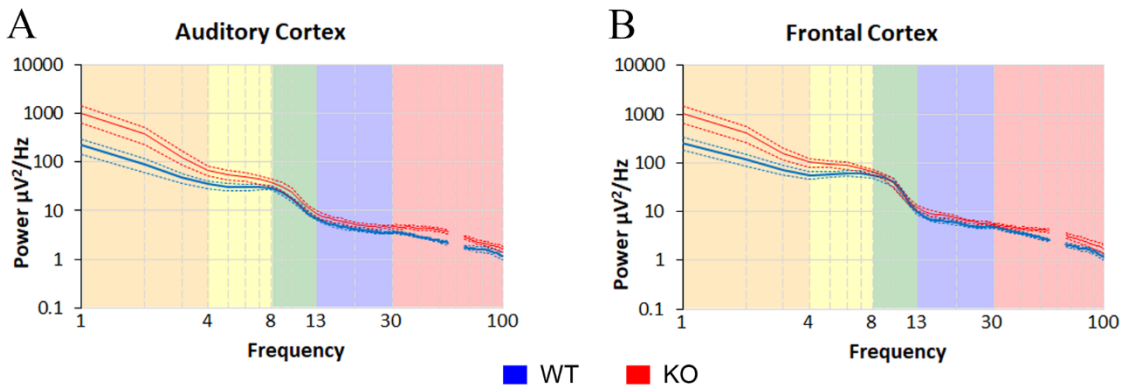

Supplemental Figure 1-1. Characterization of oscillatory EEG patterns in *Fmr1* KO and WT mice. Resting data was collected for 5 min (no auditory stimulus) and was divided into 2-sec segments. Power density ($\mu V^2/Hz$) was calculated for each artifact-free segment using Fast Fourier Transforms (FFT) in the auditory and frontal cortex. All segments for a given animal were then averaged and the individual averages then contributed to the genotype averages seen in A and B. Note: frequencies from 55 to 65 Hz were excluded in all analysis, as a 60 Hz notch filter was used to eliminate line noise.

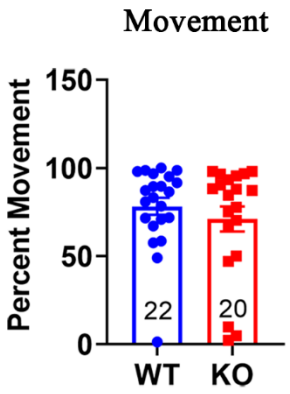

Supplemental Figure 1-2. Percent movement in WT and *Fmr1* KO mice prior to treatment. Percent movement during EEG resting baseline for WT and *Fmr1* KO mice before treatment. Statistical analysis of WT and *Fmr1* KO mice with student's t-test shows no significant difference ($t(40)=0.85$, $p=0.399$)). For EEG power coupling comparisons, animals that moved less than five percent during the resting baseline were excluded from analysis (WT N=1, KO N=2).

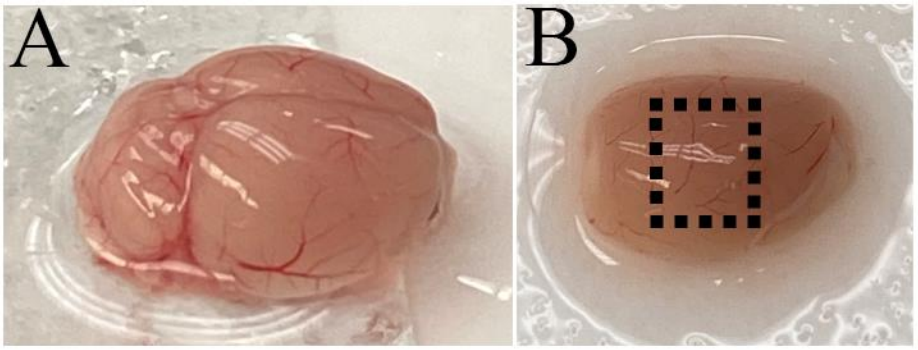

Supplemental Figure 2-1. Dissection of auditory cortex. To dissect out the auditory cortex, the brain was removed and placed on ice-cold PBS with phosphatase and protease inhibitors. The cerebellum was removed, the brain was cut along the sagittal plane to separate the two hemispheres, and the hippocampus was removed. The remaining cortex was cut to isolate the auditory cortex and surrounding cortical structures. Following isolation of cortex, underlying structures were removed.

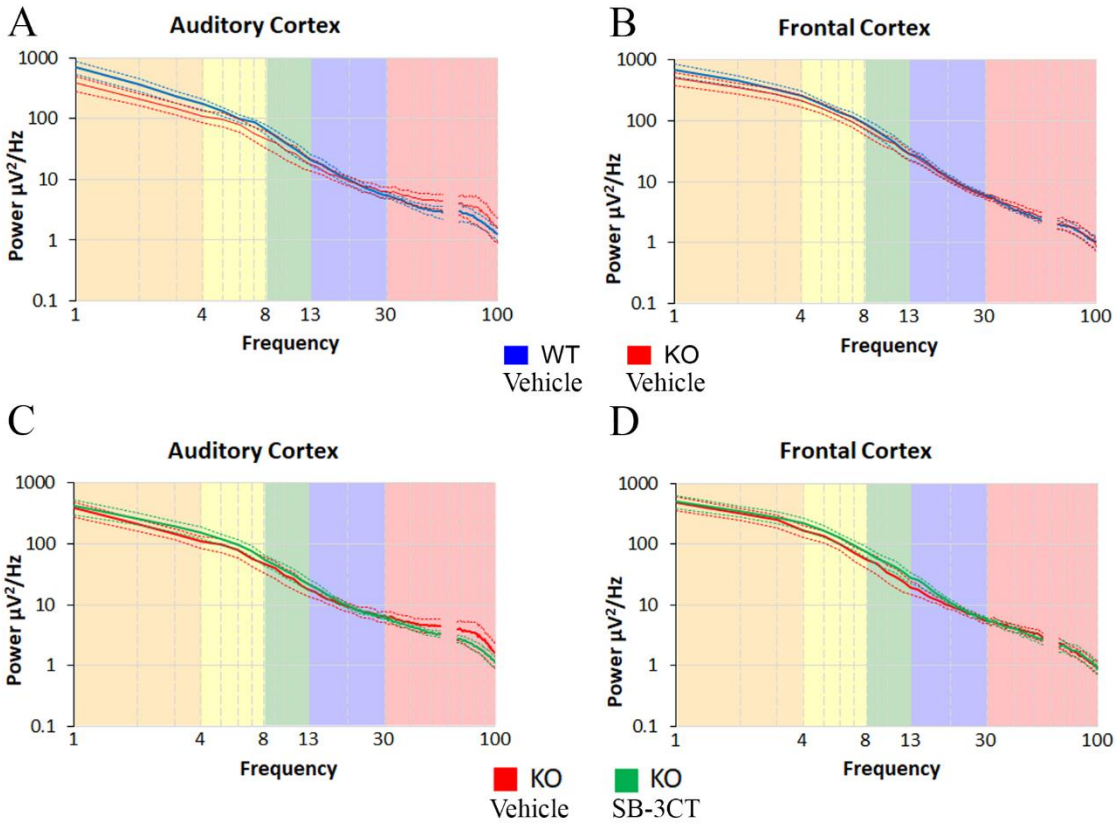

Supplemental Figure 2-2. Characterization of oscillatory EEG patterns in vehicle-treated and SB-3CT-treated *Fmr1* KO and WT mice. Resting data was collected for 5 min (no auditory stimulus) and was divided into 2-sec segments. Power density (μV^2/Hz) was calculated for each artifact-free segment using Fast Fourier Transforms (FFT) in the auditory and frontal cortex. All segments for a given animal were then averaged and the individual averages then contributed to the genotype x treatment averages seen in A-D.

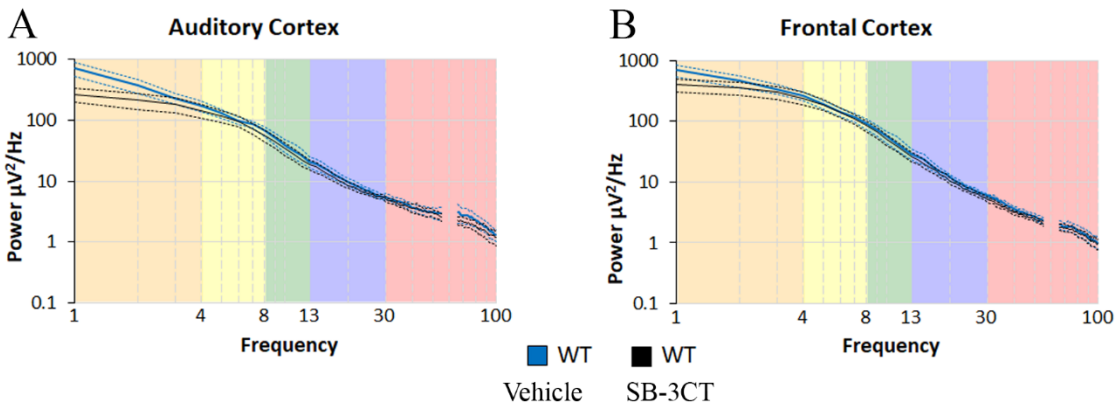

Supplemental Figure 2-3. Characterization of oscillatory EEG patterns in vehicle-treated and SB-3CT-treated WT mice. Resting data was collected for 5 min (no auditory stimulus) and was divided into 2-sec segments. Power density (μV^2/Hz) was calculated for each artifact-free segment using Fast Fourier Transforms (FFT) in the auditory and frontal cortex. All segments for a given animal were then averaged and the individual averages then contributed to the averages seen in A and B.

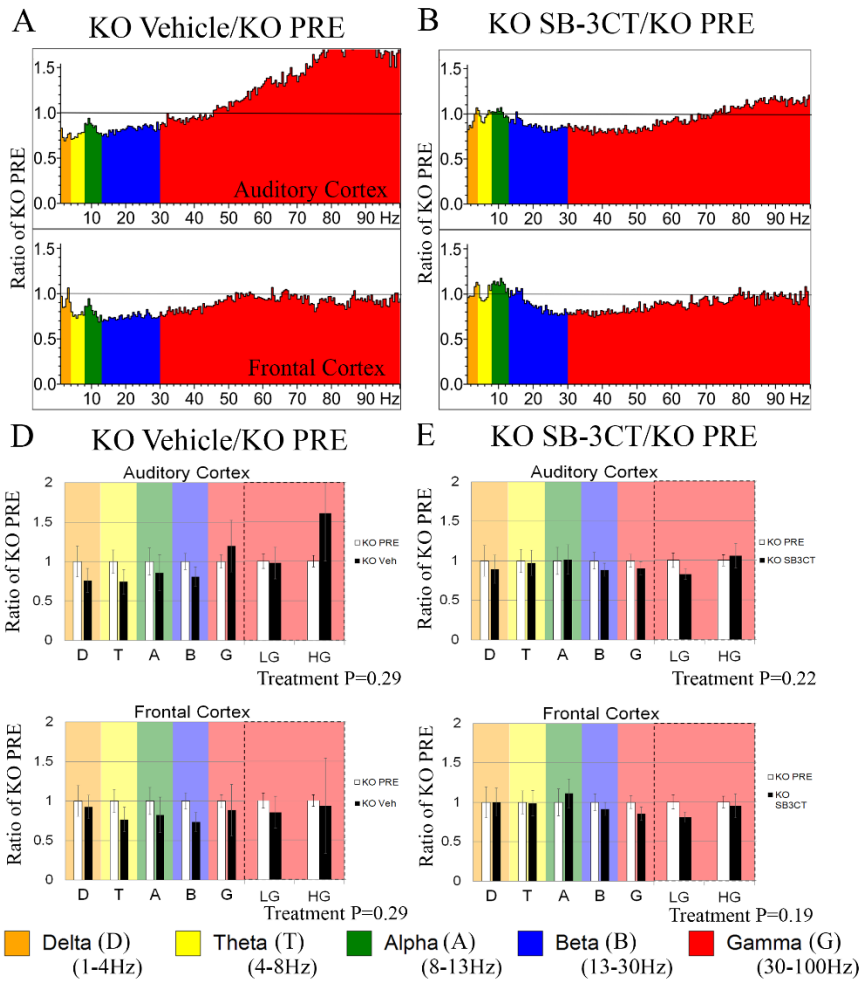

Supplemental Figure 2-4. Comparisons of vehicle- and SB-3CT-treated *Fmr1* KO mice to *Fmr1* KO PRE mice. Five minutes of resting EEG activity was recorded from electrodes implanted in the auditory (AC) and frontal cortex (FC) of vehicle-treated (A) and SB-3CT-treated (B) *Fmr1* KO mice. (D, E) Graphs show FFT calculated spectral power as a ratio of the *Fmr1* KO control group (PRE, N=20) depicted in Figure 1. One-way MANCOVA analysis of *Fmr1* KO comparisons did not reveal any significant differences in any of the frequency bands in both the AC and FC. A value of 1 indicates no mean difference in power between *Fmr1* KO treated and *Fmr1* KO control, while values above the black line indicate *Fmr1* KO treated > *Fmr1* KO control, and below indicates *Fmr1* KO treated < *Fmr1* KO control.

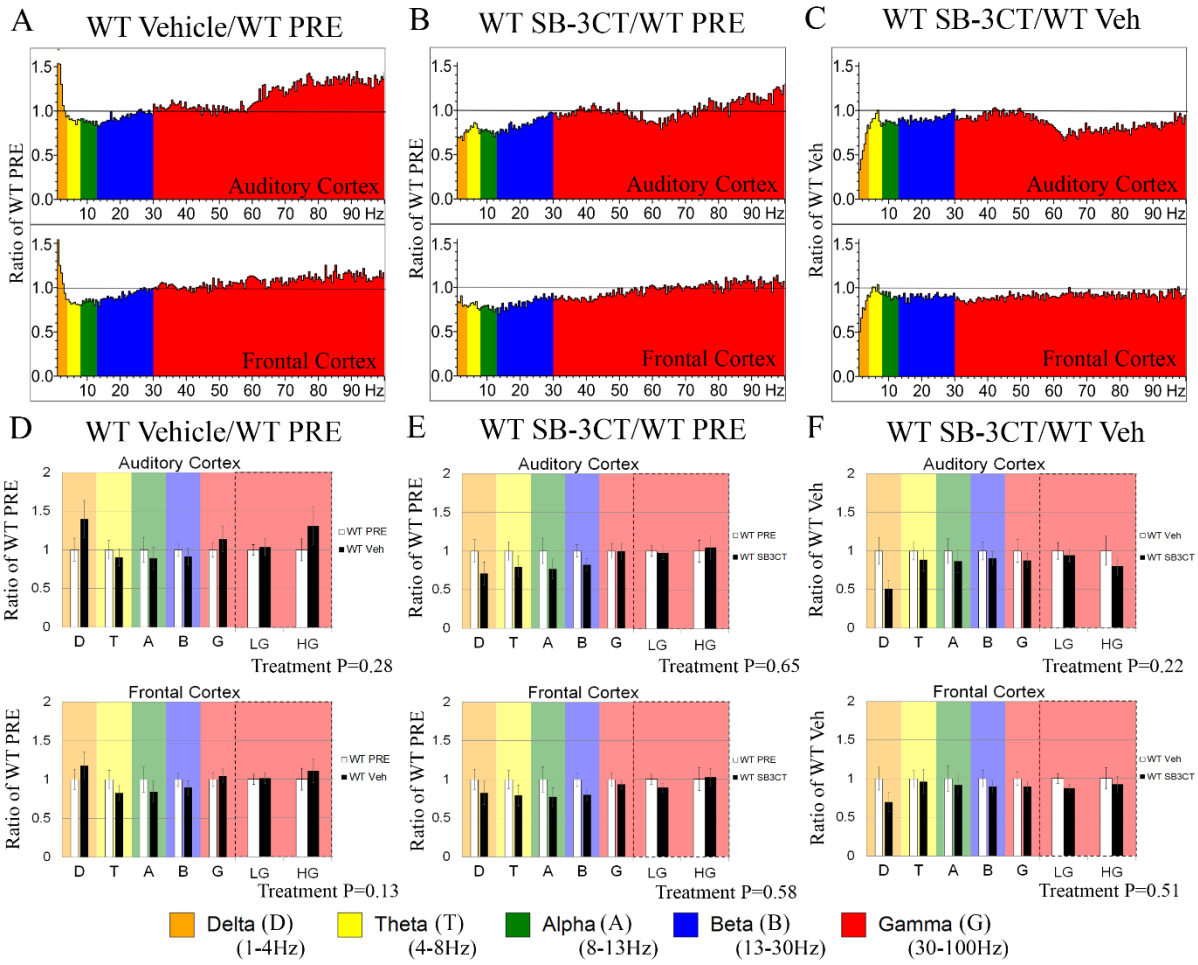

Supplemental Figure 2-5. Acute MMP-9 inhibition does not significantly alter resting gamma power in WT mice. Five minutes of resting EEG activity was recorded from electrodes implanted in the auditory (AC) and frontal cortex (FC) of WT and *Fmr1* KO mice. (A, B, D, E) Graphs show FFT calculated spectral power as a ratio of the WT control group (PRE, N=22) depicted in Figure 1. (A, D) Average power of vehicle-treated WT (N=16) mice in the AC (top) and FC (bottom). (B, E) Average power of SB-3CT-treated WT (N=15) mice. (C) Average power of SB-3CT-treated WT (N=15) mice compared to vehicle-treated WT (N=16) mice. One-way MANCOVA analysis of WT comparisons did not reveal any significant differences in any of the frequency bands in both the AC and FC. A value of 1 indicates no mean difference in power between WT treated and WT control, while values above the black line indicate WT treated > WT control, and below indicates WT treated < WT control.

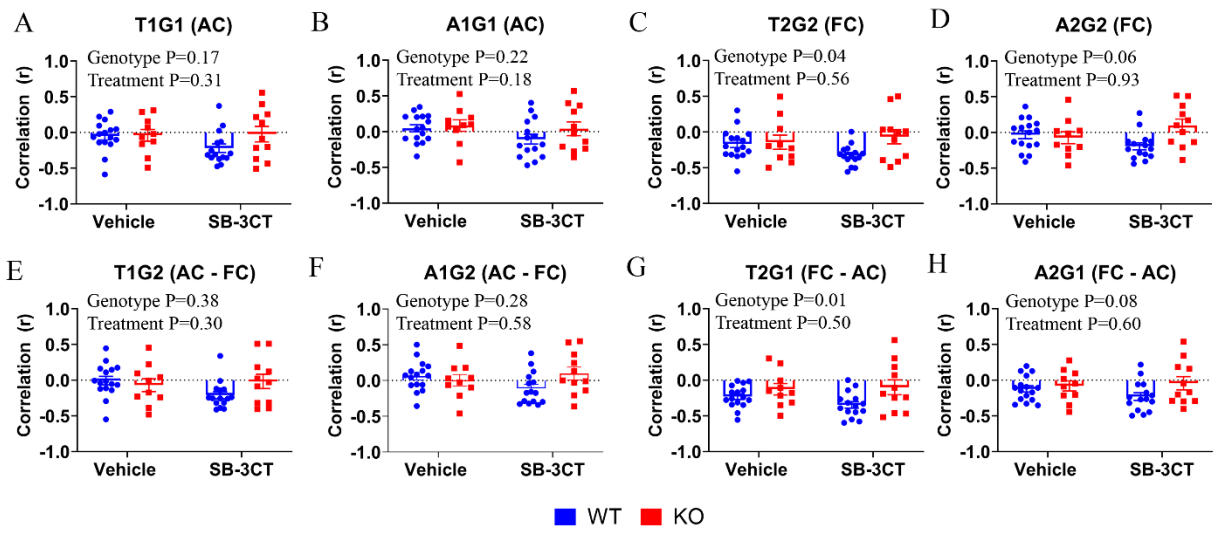

Supplemental Figure 2-6. Theta/LowGamma and Alpha/LowGamma EEG power coupling in AC and FC for treatment groups. (A-D) Graphs show the Theta/LowGamma (TG) and Alpha/LowGamma (AG) EEG power coupling for WT and *Fmr1* KO mice treated with vehicle or SB-3CT in the auditory cortex (represented by 1) and frontal cortex (represented by 2). (E-H) Graphs show cross EEG power coupling between the auditory cortex (1) and frontal cortex (2) for WT and *Fmr1* KO mice treated with vehicle or SB-3CT. Statistical analysis with two-way ANOVA for Theta/LowGamma and Alpha/LowGamma in the AC reveals no significant main effect of genotype (T1G1: $F(1,48)=1.921$, $p=0.17$; A1G1: $F(1,48)=1.578$, $p=0.22$), treatment (T1G1: $F(1,48)=1.054$, $p=0.31$: A1G1: $F(1,48)=1.833$, $p=0.18$) or interaction (T1G1: $F(1,48)=1.58$, $p=0.21$; A1G1: $F(1,48)=0.53$, $p=0.47$), respectively. Statistical analysis with two-way ANOVA for Theta/LowGamma in the FC reveals a significant main effect of genotype (T2G2: $F(1,48)=4.104$, $p=0.04$), but no significant main effect of treatment (T2G2: $F(1,48)=0.353$, $p=0.56$) or interaction (T2G2: $F(1,48)=2.843$, $p=0.10$). Statistical analysis with two-way ANOVA for Alpha/LowGamma in the FC revealed a significant interaction (A2G2: $F(1,48)=5.997$, $p=0.02$), but no main effect of genotype (A2G2: ($F(1,48)=3.468$, $p=0.07$) or main effect of treatment (A2G2: $F(1,48)=0.008$, $p=0.93$). Statistical analysis with two-way ANOVA for cross region Theta/LowGamma and Alpha/LowGamma coupling in the AC to FC reveals no significant main effect of genotype (T1G2: $F(1,48)=0.777$, $p=0.38$; A1G2: $F(1,48)=1.21$, $p=0.28$), treatment (T1G2: $F(1,48)=1.11$, $p=0.30$: A1G2: $F(1,48)=0.31$, $p=0.58$) or interaction (T1G2: $F(1,48)=3.15$, $p=0.08$; A1G2: $F(1,48)=3.71$, $p=0.06$), respectively. Statistical analysis with two-way ANOVA for cross region Theta/LowGamma coupling from FC to AC reveals a significant main effect of genotype (T2G1: $F(1,48)=7.12$, $p=0.01$), but no main effect of treatment (T2G1: $F(1,48)=0.45$, $p=0.50$) or interaction (T2G1: $F(1,48)=1.19$, $p=0.28$). Statistical analysis with two-way ANOVA for cross region Alpha/LowGamma coupling from FC to AC reveals no significant main effect of genotype (A2G1: $F(1,48)=3.163$, $p=0.08$), treatment (A2G1: $F(1,48)=0.29$, $p=0.59$), or interaction (A2G1: $F(1,48)=1.30$, $p=0.26$). For EEG power coupling comparisons, animals that moved less than five percent during the resting baseline were excluded from analysis (KO Veh N=2, KO SB N=1).

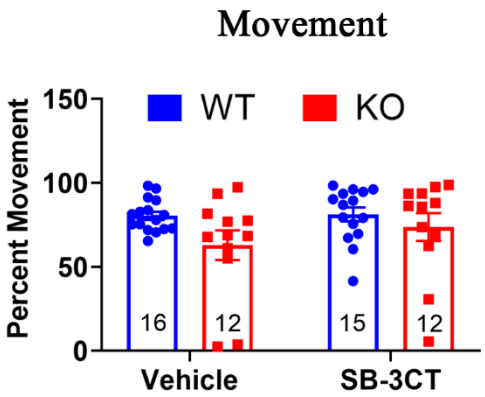

Supplemental Figure 2-7. Percent movement for vehicle-treated and SB-3CT WT and *Fmr1* KO mice. Graph shows percent movement during EEG resting baseline for WT and *Fmr1* KO mice following treatment. Statistical analysis of treatment groups with two-way ANOVA revealed a significant genotype effect ($F(1,51) = 4.46$, $p=0.04$), but no significant treatment ($F(1,91)=0.97$, $p=0.33$) or interaction effect ($F(1,51)=0.72$, $p=0.40$). *Post hoc* analysis with Bonferroni's multiple comparisons test did not reveal any significant differences between groups. For EEG power coupling comparisons, animals that moved less than five percent during the resting baseline were excluded from analysis (KO Veh N=2, KO SB N=1).

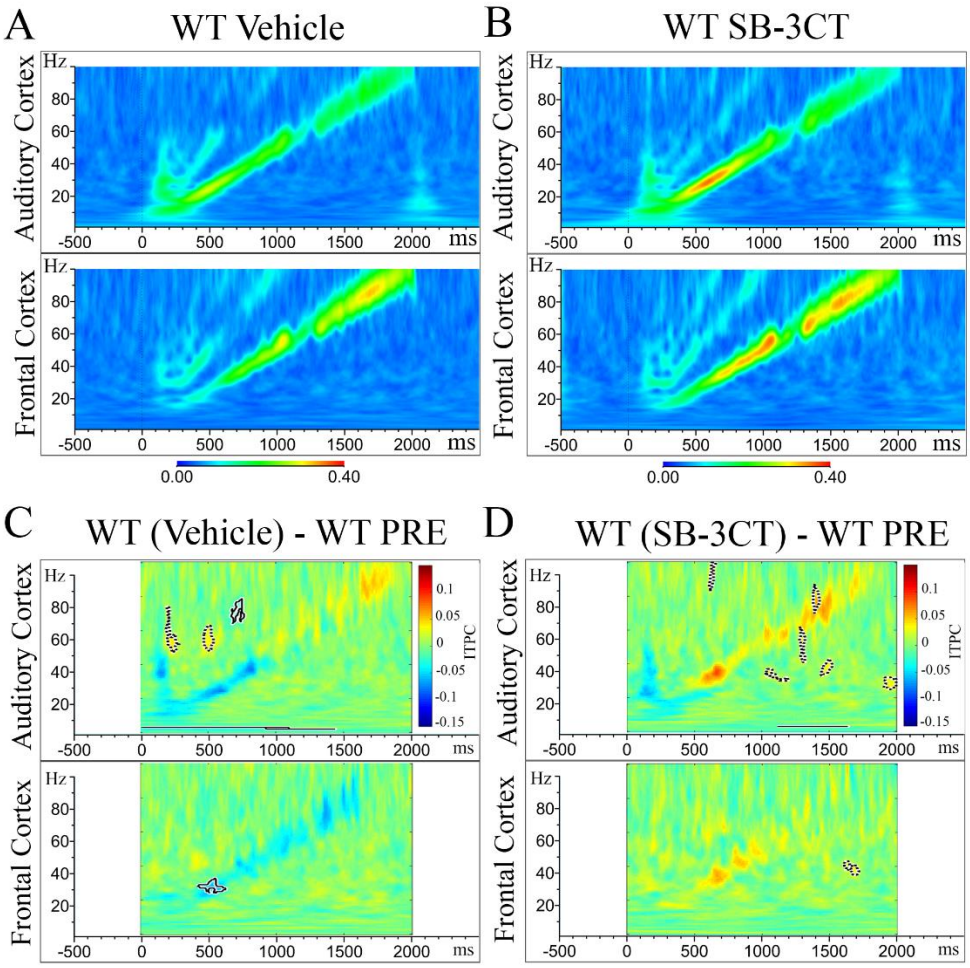

Supplemental Figure 4-1. Acute SB-3CT treatment does not significantly alter ITPC to auditory "Up Chirp" stimuli in WT mice. (A, B) Up chirp stimuli grand average ITPC in the AC (top) and FC (bottom) of vehicle-treated (N=17) and SB-3CT-treated (N=14) WT mice, respectively. Warmer colors, yellow/red, represent high ITPC values, while cooler colors, blue/green, represents low ITPC values. (C) Difference between vehicle-treated WT mice (N=17) and WT PRE (N=23) average chirp ITPC values in AC and FC. Blue areas indicate WT Veh <WT PRE, green areas represent no difference, and yellow areas WT Veh >WT PRE. (D) Difference between SB-3CT-treated WT (N=14) mice and WT PRE (N=23) average chirp ITPC values in AC and FC. For statistical analysis, clusters of p-values were calculated, and these differences were overlaid on the chirp response to demonstrate quantitative differences between each treatment group after correction for multiple comparisons. Using Monte Carlo statistical method on cluster analysis no significant differences were detected in AC or FC for average up chirp ITPC values between vehicle-treated WT (N=17) mice and WT PRE (N=23) mice (C). SB-3CT-treated WT (N=14) mice exhibited a significant increase in ITPC in high gamma band ITPC in the AC from 70-90Hz, but not FC compared to WT PRE (N=23) mice (D). Significantly different time x frequency bands between treatment groups are highlighted in bolded black lines. Similar patterns and statistics of ITPC were observed for both up and down chirps.

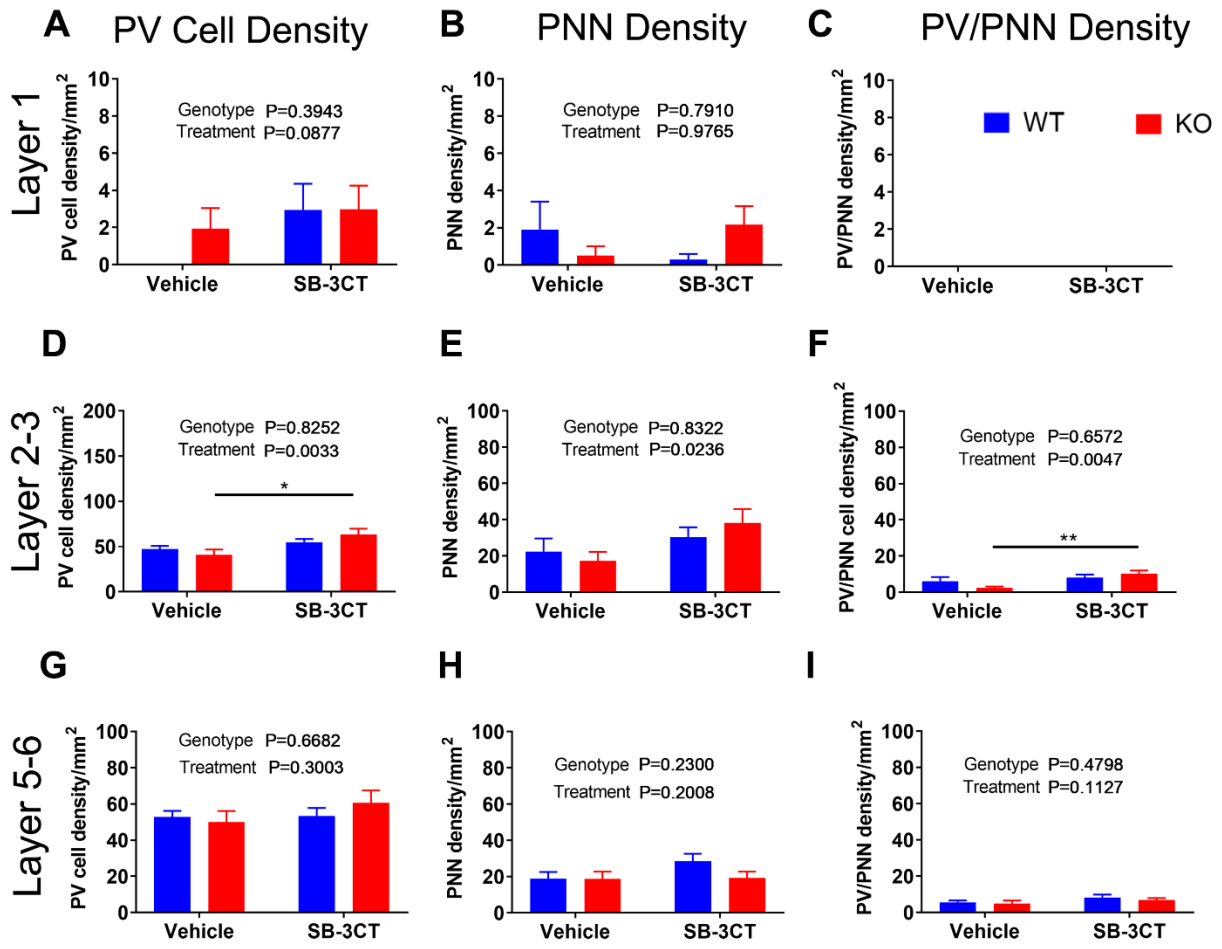

Supplemental Figure 5-1. PV/PNN quantification in auditory cortex. (A, D, G) Graphs show PV cell density in Layer 1, Layer 2-3, and Layer 5-6 of the auditory cortex. Statistical analysis reveals no significant differences in Layer 1. (B, E, H) Graphs show PNN density in Layer 1, Layer 2-3, and Layer 5-6 of the auditory cortex. Statistical analysis of PV, PNN density and PV/PNN colocalization in Layer 2-3 of the auditory cortex revealed a significant effect of treatment (PV: $F(1,74)=9.23$, $p=0.003$; PNN: $F(1,74)=5.34$, $p=0.02$; PV/PNN: $F(1,74)=8.50$, $p=0.005$), but no significant effect of genotype (PV: $F(1,74)=0.05$, $p=0.83$; PNN: $F(1,74)=0.05$, $p=0.83$; PV/PNN: $F(1,74)=0.20$, $p=0.66$) or interaction (PV: $F(1,74)=2.31$, $p=0.13$; PNN: $F(1,74)=1.08$, $p=0.30$; PV/PNN: $F(1,74)=3.18$, $p=0.08$). Statistical analysis of PV density and PV/PNN colocalization revealed a significant increase in SB-3CT-treated WT mice compared to vehicle-treated WT mice (Two-way ANOVA, $p=0.01$ (PV), $p=0.009$ (PV/PNN), $N=6$ per group). (C, F, I) Graphs show PV/PNN colocalization in Layer 1, Layer 2-3, and Layer 5-6 of the auditory cortex. Statistical analysis reveals no significant differences in Layer 5-6 of the auditory cortex. All graphs represent average values and the error bars indicate SEM.

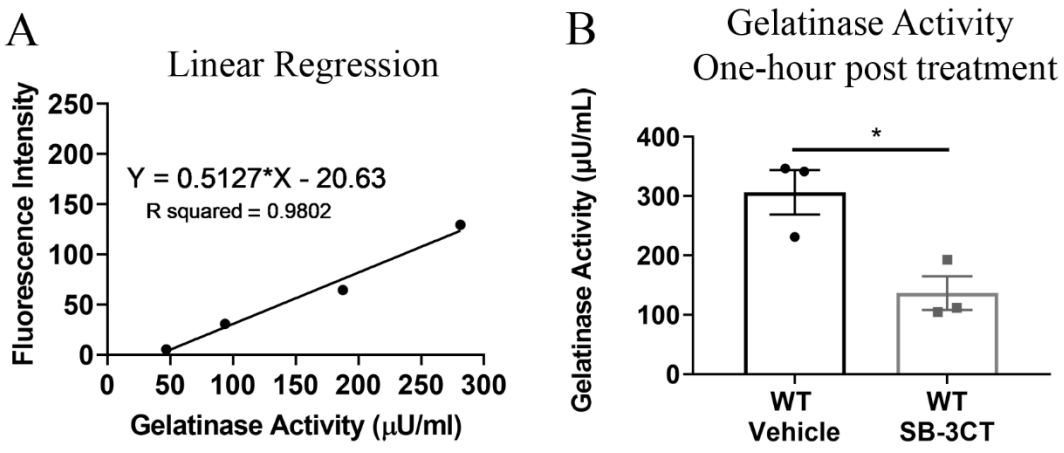

Supplemental Figure 7-1. SB-3CT inhibits gelatinase activity one-hour post treatment in WT mice. To confirm that the MMP-2/9 inhibitor, SB-3CT, reduced MMP-2/9 activity following treatment, gelatinase activity assay was measured using a Dye-Quenched gelatin assay. WT mice were injected intraperitoneally with SB-3CT (25 mg/kg) or vehicle and the auditory and surrounding cortices were collected and homogenized for the DQ gelatin assay one-hour post injection. (A) A mouse recombinant MMP-9 (specific activity approximately 1,500 pmol/min/μg) was used as a standard to obtain a readout of the approximate MMP-9 activity in the sample using a linear regression curve. (B) Graph show gelatinase activity in the cortices of vehicle-treated and SB-3CT-treated WT (C, N=3 per group, t-test, p=0.02) mice 1 h post injection.

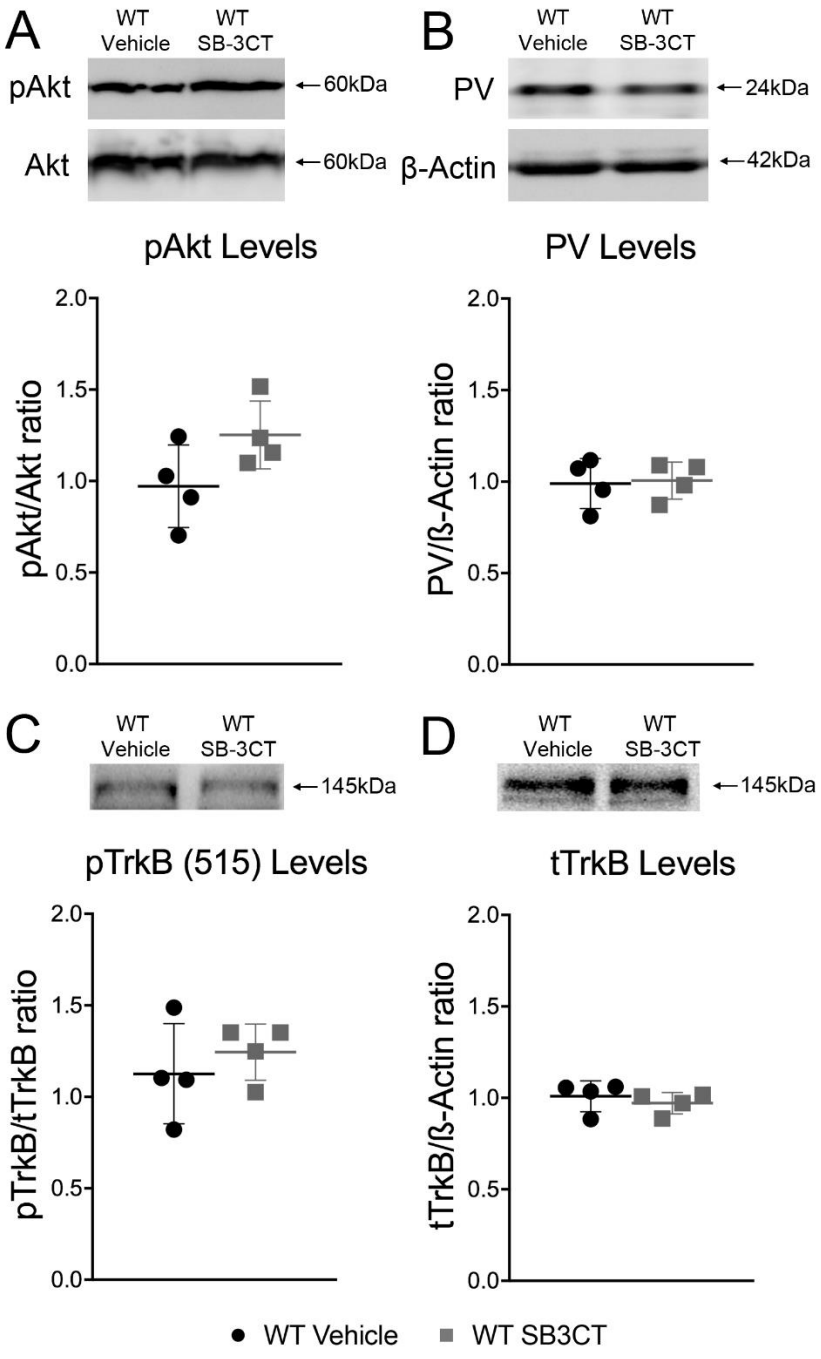

Supplemental Figure 7-2. Acute MMP-9 inhibition does not alter PV levels or phosphorylation of Akt/mTOR, and TrkB in the AC of WT mice. Western blots show levels of pAkt and Akt (A), PV and actin (B), pTrkB (Y515) (C) and total TrkB (D). Graphs show pAkt/Akt (A), PV/actin (B), pTrkB (Y515)/TrkB (C) and TrkB/actin (D) ratios in the auditory cortex of vehicle-treated and SB-3CT-treated WT mice (N=4 per group). All graphs represent average values and error bars indicate SEM.

Supplemental Table 1. Summary table of EEG resting baseline power (μV^2/Hz) for WT and *Fmr1* KO mice prior to treatment shown in Figure 1D (mean ± SEM).

Auditory Cortex (Figure 1F, top)

Genotype	Delta	Theta	Alpha	Beta	Gamma	Low Gamma	High Gamma
WT (N=22)	1.000 ± 0.149	1.000 ± 0.119	1.000 ± 0.161	1.000 ± 0.080	1.000 ± 0.094	1.000 ± 0.070	1.000 ± 0.140
KO (N=20)	1.043 ± 0.204	0.855 ± 0.125	0.788 ± 0.134	1.054 ± 0.109	1.306 ± 0.106	1.4154 ± 0.129 * (p=0.003)	1.145 ± 0.083

Frontal Cortex (Figure 1F, bottom)

Genotype	Delta	Theta	Alpha	Beta	Gamma	Low Gamma	High Gamma
WT (N=22)	1.000 ± 0.131	1.000 ± 0.120	1.000 ± 0.164	1.000 ± 0.088	1.000 ± 0.087	1.000 ± 0.063	1.000 ± 0.145
KO (N=20)	0.890 ± 0.163	0.716 ± 0.111	0.651 ± 0.107	0.925 ± 0.095	1.290 ± 0.100	1.328 ± 0.101 * (p=0.005)	1.210 ± 0.135

Auditory cortex (Figure 1G)

Genotype	**T1G1**	**A1G1**
WT (N=21)	**-0.214** ± 0.040	**-0.142** ± 0.042
***Fmr1* KO (N=18)**	**-0.052** ± 0.057 * (p=0.02)	**0.050** ± 0.056 ** (p=0.008)

Frontal Cortex (Figure 1H)

Genotype	**T2G2**	**A2G2**
WT (N=21)	**-0.290** ± 0.041	**-0.214** ± 0.045
***Fmr1* KO (N=18)**	**-0.146** ± 0.065, (p=0.06)	**-0.068** ± 0.063, (p=0.06)

Auditory to Frontal Cortex (Figure 1I)

Genotype	**T1G2**	**A1G2**
WT (N=21)	**-0.207** ± 0.044	**-0.130** ± 0.045
***Fmr1* KO (N=18)**	**-0.036** ± 0.061 * (p=0.03)	**0.016** ± 0.053 * (p=0.04)

Frontal to Auditory Cortex (Figure 1J)

Genotype	**T2G1**	**A2G1**
WT (N=21)	**-0.323** ± 0.032	**-0.261** ± 0.030

***Fmr1* KO (N=18)**	**-0.182** ± 0.061 * (p=0.04)	**-0.114** ± 0.063 * (p=0.03)

Supplemental Table 2. Summary table of EEG resting baseline power (μV^2/Hz) for WT and *Fmr1* KO mice post treatment with SB-3CT (25mg/kg) or vehicle shown in Figure 2D, 2E, 2F (mean ± SEM).

Auditory cortex (Figure 2D)

Genotype	Delta	Theta	Alpha	Beta	Gamma	Low Gamma	High Gamma
KO Vehicle (N=12)	0.567 ± 0.112	0.702 ± 0.147	0.761 ± 0.201	0.936 ± 0.140	1.371 ± 0.376	1.335 ± 0.273	1.406 ± 0.530
WT Vehicle (N=16)	1.000 ± 0.173	1.000 ± 0.120	1.000 ± 0.162	1.000 ± 0.116	1.000 ± 0.145	1.000 ± 0.107	1.000 ± 0.188

Frontal cortex

Genotype	Delta	Theta	Alpha	Beta	Gamma	Low Gamma	High Gamma
KO Vehicle (N=12)	0.698 ± 0.131	0.661 ± 0.129	0.637 ± 0.175	0.762 ± 0.087	1.088 ± 0.130	1.115 ± 0.125	1.018 ± 0.151
WT Vehicle (N=16)	1.000 ± 0.150	1.000 ± 0.112	1.000 ± 0.163	1.000 ± 0.104	1.000 ± 0.087	1.000 ± 0.064	1.000 ± 0.136

Auditory cortex (Figure 2E)

Genotype	Delta	Theta	Alpha	Beta	Gamma	Low Gamma	High Gamma
KO SB-3CT (N=12)	1.313 ± 0.262	1.043 ± 0.174	1.047 ± 0.120	1.135 ± 0.107	1.184 ± 0.110	1.194 ± 0.096	1.157 ± 0.166
WT SB-3CT (N=15)	1.000 ± 0.207	1.000 ± 0.164	1.000 ± 0.169	1.000 ± 0.098	1.000 ± 0.101	1.000 ± 0.090	1.000 ± 0.144

Frontal cortex

Genotype	Delta	Theta	Alpha	Beta	Gamma	Low Gamma	High Gamma
KO SB-3CT (N=12)	1.078 ± 0.198	0.889 ± 0.161	0.935 ± 0.172	1.053 ± 0.105	1.172 ± 0.149	1.20 ± 0.132	1.121 ± 0.202
WT SB-3CT (N=15)	1.000 ± 0.184	1.000 ± 0.160	1.000 ± 0.150	1.000 ± 0.092	1.000 ± 0.063	1.000 ± 0.059	1.000 ± 0.109

Auditory cortex (Figure 2F)

Genotype	Delta	Theta	Alpha	Beta	Gamma	Low Gamma	High Gamma
KO SB-3CT (N=12)	1.174 ± 0.234	1.312 ± 0.219	1.188 ± 0.215	1.094 ± 0.103	0.757 ± 0.070	0.845 ± 0.068	0.660 ± 0.095

KO Vehicle (N=12)	1.000 ± 0.120	1.000 ± 0.209	1.000 ± 0.264	1.000 ± 0.149	1.000 ± 0.275	1.000 ± 0.205	1.000 ± 0.377

Frontal cortex

Genotype	Delta	Theta	Alpha	Beta	Gamma	Low Gamma	High Gamma
KO SB-3CT (N=12)	1.081 ± 0.199	1.291 ± 0.234	1.350 ± 0.248	1.241 ± 0.124	0.966 ± 0.123	0.944 ± 0.104	1.018 ± 0.183
KO Vehicle (N=12)	1.000 ± 0.187	1.000 ± 0.195	1.000 ± 0.274	1.000 ± 0.114	1.000 ± 0.119	1.000 ± 0.113	1.000 ± 0.148

Supplemental Table 3. Summary table showing density of PV cells, WFA+ PNNs, PV/PNN co-localization, and PNN+/PV- cells in the layer 4 of the auditory cortex of WT and *Fmr1* KO mice post treatment with SB-3CT (25mg/kg) or vehicle shown in Figure 5 (mean ± SEM).

	WT Vehicle (n=18)	WT SB-3CT (n=23)	*Fmr1* KO Vehicle (n=20)	*Fmr1* KO SB-3CT (n=17)
PV+ cell density (N=6)	92.45 ± 4.60	103.09 ± 7.31 * (p=0.0215)	78.09 ± 5.11	99.05 ± 7.01
PNN+ density (N=6)	99.71 ± 11.16	142.50 ± 8.78 ** (p=0.0096), * (p=0.03)	64.15 ± 10.05 **** (p<0.0001)	104.74 ± 7.46 * (p=0.02)
PV+/PNN+ colocalization (N=6)	38.17 ± 4.10	56.17 ± 5.75 * (p=0.04)	27.51 ± 4.28 *** (p=0.0002)	50.55 ± 4.24 ** (p=0.009)
PNN+ / PV- (N=6)	61.53 ± 8.65	86.32 ± 7.18 **** (p<0.0001)	36.65 ± 6.36	54.19 ± 7.50 * (p=0.02)

Supplemental Table 4. Statistical results for Layer 4 auditory cortex PV/PNN analysis (Figure 5). All analysis was performed using two-way ANOVA.

	Genotype	Treatment	Interaction
PV+ cell density (N=6)	F(1,74) = 2.12, p=0.15	F(1,74) = 6.262, p=0.01	F(1,74)=0.67, p=0.42
PNN+ density (N=6)	F(1,74)=14.64, p=0.0003	F(1,74)=18.94, P<0.0001	F(1,74)=0.013, p=0.909
PV+/PNN+ colocalization (N=6)	F(1,74)=2.8, p=0.09	F(1,74)=17.78, p<0.0001	F(1,74)=0.268, p=0.606
PNN+ / PV- (N=6)	F(1,74)=14.53, p=0.0003	F(1,74)=8.00, p=0.006	F(1,74)=0.23, p=0.63

Supplemental Table 5. Summary table showing locomotor activity, anxiety, and hyperactivity measures for WT and *Fmr1* KO mice during elevated plus maze (EPM) and open field (OF) behavior tests shown in Figure 6A-H (mean ± SEM).

	WT Vehicle	WT SB-3CT	*Fmr1* KO Vehicle	*Fmr1* KO SB-3CT
Total Entries (EPM)	28.30 ± 2.86	31.38 ± 3.12	44.13 ± 3.01 **** (p<0.0001)	28.29 ± 2.97 ### (p=0.0001)
Speed (EPM)	26.04 ± 1.96	28.59 ± 2.14	33.64 ± 2.07 ** (p=0.003)	24.31 ± 2.04 ### (p=0.0008)
% Time in open arms (EPM)	69.50 ± 3.89	73.38 ± 4.25	43.13 ± 4.10 **** (p<0.0001)	72.79 ± 4.04 ####(p<0.0001)
Total line crosses (OF)	212.80 ± 15.40	232.30 ± 16.80	300.90 ± 16.20 **** (p<0.0001)	203.40 ± 16.00 ####(p<0.0001)
Speed (OF)	45.52 ± 3.73	50.98 ± 4.07	69.79 ± 3.93 **** (p<0.0001)	53.52 ± 3.87 ## (p=0.002)
Time spent in center/entry (OF)	0.93 ± 0.13	0.93 ± 0.14	0.52 ± 0.14 * (p=0.0173)	1.01 ± 0.13 ## (p=0.008)
% Time in thigmotaxis (OF)	47.79 ± 2.81	48.80 ± 3.06	68.04 ± 2.96 **** (p<0.0001)	50.21 ±2.92 ####(p<0.0001)
Center entries (OF)	6.00 ± 1.28	6.50 ± 1.40	2.30 ± 1.35 * (p=0.03)	7.00 ± 1.33 # (p=0.01)

Supplemental Table 6. Statistical results for locomotor activity, anxiety, and hyperactivity measures for WT and *Fmr1* KO mice during elevated plus maze (EPM) and open field (OF) behavior tests (Figure 6). All analysis was performed using two-way ANOVA.

	Genotype	Treatment	Interaction
Total Entries (EPM)	F(1,29) = 9.07, p=0.0053	F(1,29) = 9.11, p=0.0053	F(1,29) = 20, p=0.0001
Speed (EPM)	F(1,29) = 1.308, p=0.2620	F(1,29) = 5.452, p=0.0267	F(1,29) = 16.79, p=0.0003
% Time in open arms (EPM)	F(1,29) = 21.93, p<0.0001	F(1,29) = 33.92, p<0.0001	F(1,29) = 20.05, p=0.0001
Total line crosses (OF)	F(1,29) = 6.756, p=0.0145	F(1,29) = 11.71, p=0.0019	F(1,29) = 26.3, p<0.0001
Speed (OF)	F(1,29) = 26.33, p<0.0001	F(1,29) = 4.961, p=0.0341	F(1,29) = 17.71, p=0.0002
Time spent in center/entry (OF)	F(1,29) = 3.039, p=0.919	F(1,29) = 6.498, p=0.0163	F(1,29) = 6.533, p=0.0161
% Time in thigmotaxis (OF)	F(1,29) = 27.18, p<0.0001	F(1,29) = 16.38, p=0.0004	F(1,29) = 20.55, p<0.0001
Center entries (OF)	F(1,29) = 2.939, p=0.0972	F(1,29) = 7.668, p=0.0097	F(1,29) = 5.025, p=0.0328

Supplemental Table 7. Summary table showing gelatinase activity in the auditory cortex of WT and *Fmr1* KO mice one-hour post vehicle or SB-3CT (25mg/kg) treatment shown in Figure 7C (mean ± SEM).

	KO Vehicle	KO SB-3CT

Gelatinase Activity (µU/mL)	167.4 ± 23.69	33.87 ± 36.58 * (p=0.02)
	WT Vehicle	WT SB-3CT
Gelatinase Activity (µU/mL)	306.3 ± 37.64	136.4 ± 28.36 * (p=0.02)

Supplemental Table 8. Summary table showing protein levels in the auditory cortex of *Fmr1* KO mice one-hour post vehicle or SB-3CT (25mg/kg) treatment shown in Figure 7A-D (mean ± SEM).

	KO Vehicle (N=4)	KO SB-3CT (N=4)
PV levels	0.96 ± 0.07	1.44 ± 0.15 * (p-0.04)
p-Akt/Akt ratio	1.29 ± 0.08	0.76 ± 0.09 * (p=0.02)
p-TrkB(515)/TrkB ratio	1.00 ± 0.02	1.39 ± 0.12 * (p=0.03)
TrkB levels	1.00 ± 0.08	0.89 ± 0.06